0026-895X/08/7404-964–971$20.00
MOLECULAR PHARMACOLOGY
Copyright © 2008 The American Society for Pharmacology and Experimental Therapeutics
Mol Pharmacol 74:964–971, 2008

Vol. 74, No. 4
43661/3384206
Printed in U.S.A.

Functional Role of Arginine 375 in Transmembrane Helix 6 of Multidrug Resistance Protein 4 (MRP4/ABCC4)

Azza A. K. El-Sheikh, Jeroen J. M. W. van den Heuvel, Elmar Krieger, Frans G. M. Russel, and Jan B. Koenderink

Department of Pharmacology and Toxicology (A.A.K.E., J.J.M.W.v.d.H., F.G.M.R., J.B.K.) and Centre for Molecular and Biomolecular Informatics (E.K.), Radboud University Nijmegen Medical Centre, Nijmegen Centre for Molecular Life Sciences, Nijmegen, The Netherlands

Received November 20, 2007; accepted July 8, 2008

ABSTRACT

Multidrug resistance protein (MRP) 4 transports a variety of endogenous and xenobiotic organic anions. MRP4 is widely expressed in the body and specifically localized to the renal apical proximal tubule cell membrane, where it mediates the excretion of these compounds into urine. To characterize the MRP4 substrate-binding site, the amino acids Phe^{368}, Phe^{369}, Glu^{374}, Arg^{375}, and Glu^{378} of transmembrane helix 6, and Arg^{998} of helix 12, localized in the intracellular half of the central pore, were mutated into the corresponding amino acids of MRP1 and MRP2. Membrane vesicles isolated from human embryonic kidney 293 cells overexpressing these mutants showed significantly reduced methotrexate (MTX) and cGMP transport activity compared with vesicles that expressed wild-type MRP4. The only exception was substitution of Arg^{375} with serine, which had no effect on cGMP transport but significantly decreased the affinity of MTX. Substitution of the same amino acid with a positively charged lysine returned the MTX affinity to that of the wild type. Furthermore, MTX inhibition of MRP4-mediated cGMP transport was noncompetitive, and the inhibition constant was increased by introduction of the R375S mutation. A homology model of MRP4 showed that Arg^{375} and Arg^{998} face right into the central aqueous pore of MRP4. We conclude that positively charged amino acids in transmembrane helices 6 and 12 contribute to the MRP4 substrate-binding pocket.

Proteins belonging to the ATP-binding cassette (ABC) superfamily play a crucial role in human physiology, pharmacology, and toxicology, as well as numerous pathological conditions. To date, 48 human ABC transporter proteins have been identified, including nine multidrug resistance proteins (MRPs) belonging to the C subfamily (van de Water et al., 2005). MRPs are not only important for the tumor cell resistance they confer to chemotherapeutic drugs but also for their endogenous expression in normal human tissues. MRP4/ABCC4 is widely distributed in epithelial tissue and blood cells, and highest expression has been found in kidney, lung, prostate, liver, tonsils, and bladder (Borst et al., 2007). In most epithelial cells, MRP4 is located at the basolateral membrane, except for the renal proximal tubular cell where it is expressed apically (van Aubel et al., 2002). Structurally, the human MRP4 protein consists of 1325 amino acids composed of two membrane-spanning domains each consisting of six transmembrane α-helices (TM), with two cytosolic ATP-binding domains. MRP4 mediates ATP-dependent transport of various organic anions from the intracellular to the extracellular side (Russel et al., 2008). Substrates include endogenous compounds such as the cAMP and cGMP monophosphate (van Aubel et al., 2002), folate (Chen et al., 2002), and uric acid (Van Aubel et al., 2005), as well as drugs such as the antiviral nucleoside monophosphate analog 9-(2-phosphonylmethoxyethyl)adenine (Schuetz et al., 1999) and the nucleobase analogs 6-mercaptopurine (Wielinga et al., 2002) and methotrexate (MTX) (Chen et al., 2002).

The mode by which MRPs transport their substrates has still to be identified. Among the different MRPs, the structure-function relationship of MRP1 has been investigated most extensively (Deeley et al., 2006). Several mutational studies have shown that polar amino acids in transmem-

Article, publication date, and citation information can be found at http://molpharm.aspetjournals.org.
doi:10.1124/mol.107.043661.

ABBREVIATIONS: ABC, ATP-binding cassette; MRP, multidrug resistance; TM, transmembrane α-helix(es); 8-azido-ATP-biotin, 8-azidoadenosine 5′-triphosphate 2′,3′-biotin-long-chain-hydrazone; EYFP, enhanced yellow fluorescent protein; MTX, methotrexate; PCR, polymerase chain reaction; HEK, human embryonic kidney; E-64, *N*-(*trans*-epoxysuccinyl)-L-leucine 4-guanidinobutylamide; PDB, Protein Data Bank; MDR, multidrug resistant; NBD, nucleotide-binding domain(s).

brane helices 11 and 17 of MRP1 are involved in substrate binding (Ito et al., 2001a,b; Zhang et al., 2001, 2006; Koike et al., 2004). In a model, most of their side chains were found to line the "pore" adjacent to the membrane cytosol interface. In contrast with MRP1, limited knowledge regarding the amino acids involved in substrate specificity of MRP2 (Ito et al., 2001a) and MRP3 (Zhang et al., 2003b) is available.

To date, no attempt has been made to characterize the MRP4 substrate-binding site(s). In the present study, we investigated the role of Phe^{368}, Phe^{369}, Glu^{374}, Arg^{375}, and Glu^{378} present in transmembrane helix 6 (TM11 in MRP1) and Arg^{998} in transmembrane helix 12 (TM17 in MRP1) in transport of cGMP and MTX. These amino acids are highly conserved in MRP4 among different species (Chen and Klaassen, 2004), but there is a large variety within the MRP subfamily (Fig. 1) that might point to a specific mechanistic importance of these amino acids. When they were substituted by their analogs from MRP1/MRP2, most mutations abolished MRP4 transport activity, except for Arg^{375} in which cGMP transport was preserved, whereas the affinity for MTX was reduced. We studied this mutation in more detail and developed a homology model of MRP4 to explain the results.

Materials and Methods

Materials. [3′,5′,7′-^{3}H(N)]Methotrexate sodium salt (specific activity, 51.5 Ci/mmol) and [8-^{3}H]guanosine-3′,5′-cyclic phosphate NH_4 salt (specific activity, 7.7 Ci/mmol) were purchased from Moravek Biochemicals (Brea, CA). The Bac-to-Bac Gateway system, culture medium, and Alexa Fluor 680 goat anti-rabbit IgG secondary antibody were purchased from Invitrogen (Breda, The Netherlands). Methotrexate, guanosine 3′5′-cyclic monophosphate, and GenElute Plasmid Mini-Prep kit were purchased from Sigma (Zwijndrecht, The Netherlands). Fetal bovine serum was purchased from MP Biochemicals (Amsterdam, The Netherlands). Multiscreen HTS-HV 0.45-μm, 96-well filters were obtained from Millipore (Etten-Leur, The Netherlands). Protein concentrations were determined with an assay kit from Bio-Rad Laboratories (Veenendaal, The Netherlands). 8-Azidoadenosine 5′-triphosphate 2′,3′-biotin-long-chain-hydrazone ($8N_3$ATP-2′,3′-biotin-LC-hydrazone) was purchased from Affinity Labeling Technologies (Nicholasville, KY), and streptavidin horseradish peroxidase conjugate was from GE Healthcare (Chalfont St. Giles, UK).

```
Human      LYGAVRLTVTLFFPSAIERVSEAIVSIRR
Mouse      LYGAVRLTVTLFFPSAIERGSEAIVSIRR
Rat        LYGAVRLTVTLFFPSAIERVSEAVVSVRR
Dog        LYGAVRLTVTLFFPSAIERVSESVVSIQR
Chicken    LYGAVRLTVTLFFPSAVERVSEAVVSIRR
Cow        LYGAVRLTVTLFFPSAVEKVSEAFVSIRR
Zebrafish  LYSAVRLTVTLFFPAAIEKVSESAISIRR
Platypus   LYGAVRVTVTLFFPAAVERVSETIISIRR
Opossum    LYGAVRLTVTLFFPAAVEKMSETRVSIKR
           **.***:*******:*:*: **: :*::*

MRP1       LFNILRFPLNIL-PMVISSIVQASVSLKR 615
MRP2       LFNILRFPLSML-PMMISSMLQASVSTER 612
MRP3       LFNILRLPLNML-PQLISNLTQASVSLKR 601
MRP4       LYGAVRLTVTLFFPSAIERVSEAIVSIRR 385
MRP5       VFNSMTFALKVT-PFSVKSLSEASVAVDR 466
MRP6       VLNILNKAQAFL-PFSIHSLVQARVSFDR 600
```

Fig. 1. Alignment of amino acid sequence of TM6 (TM11) of MRP4 for multiple species and human MRP1–6. The bold and underlined amino acids have been mutated in this study.

Generation of Human MRP4 Baculovirus. Full-length human MRP4 cDNA was generated as described previously (El-Sheikh et al., 2007). Briefly, the Bac-to-Bac system, normally used for protein production in insect cells, was modified for protein expression in mammalian cells by introduction of the cytomegalovirus promoter and Gateway destination elements (cassette that contains the chloramphenicol resistance gene and the ccdB gene flanked by attR1 and attR2 sites) in the pFastBacDual vector. In addition, the vesicular stomatitis virus G protein cDNA was cloned behind the P10 promoter of the pFastBacDual vector. The human MRP4 was cloned into the Gateway entry vector and transferred to the newly constructed Bac-to-Bac vector with the gateway LR reaction. Baculoviruses were produced as described in the Bac-to-Bac manual. As a negative control, enhanced yellow fluorescent protein (EYFP) was also introduced into the Baculovirus expression system (Invitrogen).

Site-Directed Mutagenesis. PCR was performed on a template pENTR-MRP4 vector using two primers (forward and reverse) produced by Biolegio (Nijmegen, The Netherlands) bearing one or more mismatched bases at the site of residues to be mutated. In this PCR reaction, *PfuUltra* II fusion HS DNA polymerase with the supplied reaction buffer, and dNTP mix (12.5 mM), each completed to 50-μl end volume, were used. PCR amplification consisted of initial denaturation at 94°C, followed by 20 cycles of denaturation at 94°C, annealing at 58°C, and elongation at 72°C for 14 min. The PCR product was cut by DpnI for 2 h at 37°C and finally transformed into

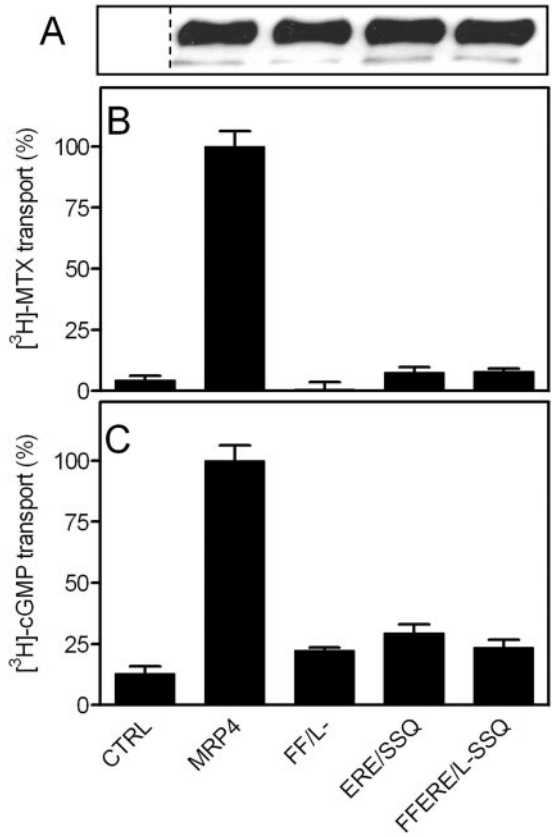

Fig. 2. Western blot analysis (A), 0.5 μM [^{3}H]MTX (B), and 1 μM [^{3}H]cGMP (C) transport activity of wild-type, FF/L-, ERE/SSQ, and FFERE/L-SSQ MRP4 transporter proteins. Top (A) represents a Western blot of membrane vesicles isolated from HEK293 cells overexpressing MRP4 or MRP4 mutants FF/L-, ERE/SSQ, and FFERE/L-SSQ as well as a negative control detected by polyclonal anti-human MRP4 (representative of three). The MRP4 wild-type transport activity for [^{3}H]MTX (950 ± 60 fmol/mg protein/min) and [^{3}H]cGMP (114 ± 7 fmol/mg protein/min) was set at 100%.

Escherichia coli DH5α cells. pENTR-MRP4 mutant plasmids were isolated using the GenElute Plasmid Mini-Prep kit (Sigma) from kanamycin-resistant colonies. All mutations were confirmed by sequencing of the full-length MRP4/ABCC4 DNA. Twelve mutants of the human MRP4 were generated: FF/L- (F368L and F369-), ERE/SSQ (E374S, R375S, and E378Q), FFERE/L-SSQ (F368L, F369-, E374S, R375S, and E378Q), F368L, F369-, E374S, R375S, R375A, R375K, R375E, E378Q, and R998A.

Transduction of MRP4 and Mutants Expression Vectors in HEK293 Cells. HEK293 cells were cultured in 182-cm^2 flasks until 40% confluent, after which the culture medium was removed and 3.5 ml of fresh medium and 1.5 ml of control EYFP, MRP4, or MRP4-mutant baculovirus was added. The cells were incubated for 15 min at 37°C, after which 20 ml of medium was added. After 24 h of transduction, 5 mM sodium butyrate was added. Three days after transduction, the cells were harvested.

Isolation of Membrane Vesicles and Protein Analysis. Cells were harvested by centrifugation at 3000*g* for 30 min. The pellets were resuspended in ice-cold homogenization buffer (0.5 mM sodium phosphate and 0.1 mM EDTA, pH 7.4) supplemented with protease inhibitors (100 μM phenylmethylsulfonyl fluoride, 5 μg/ml aprotinin, 5 μg/ml leupeptin, 1 μM pepstatin, and 1 μM E-64) and shaken at 4°C for 60 min. Lysed cells were centrifuged at 4°C at 100,000*g* for 30 min, and the pellets were homogenized in ice-cold TS buffer (10 mM Tris-HEPES and 250 mM sucrose, pH 7.4) using a tight-fitting Dounce homogenizer for 30 strokes. After centrifugation at 500*g* at 4°C for 20 min, the supernatant was centrifuged at 4°C at 100,000*g* for 60 min. The resulting pellet was resuspended in TS buffer and passed through a 27-gauge needle 30 times. Protein concentration was determined by Bio-Rad protein assay kit. Crude membrane vesicles were dispensed in aliquots, frozen in liquid nitrogen, and stored at −80°C until use.

Western Blotting. The membrane vesicle preparations (15 μg of protein) were solubilized in SDS-polyacrylamide gel electrophoresis sample buffer and separated on SDS gels containing 7.5% acrylamide according to Laemmli (1970). Subsequently, they were blotted on nitrocellulose membrane using the iBlot dry blotting system (Invitrogen). Polyclonal anti-human MRP4 rabbit serum antibody (van Aubel et al., 2002) was used to detect human MRP4 and MRP4 mutants. The secondary antibody used was the fluorescent Alexa Fluor 680 (Invitrogen). Signals were visualized with a fluorescent method, using Odyssey infrared imaging system (Li-Cor Biosciences, Lincoln, NE).

Vesicular Transport Assays. Uptake of [^{3}H]MTX or [^{3}H]cGMP into membrane vesicles was performed using a rapid filtration technique. TSB buffer (TS buffer with 0.2 mg/ml bovine serum albumin) supplemented with a mixture of 4 mM ATP and 10 mM $MgCl_2$ was added to the membrane vesicles in a final volume of 30 μl. The reaction was started when the mixture was incubated at 37°C. After 15 min, the reaction was stopped by placing samples on ice. After 1 min, 150 μl of ice-cold TSB buffer was added to each reaction well. Diluted samples were filtered by a Multiscreen HTS-Vacuum Manifold filtration device (Millipore, Etten-Leur, The Netherlands) through 0.45-μm pore, 96-well Millipore filters that were preincubated with TSB buffer. After adding 4 ml of scintillation fluid to each filter and subsequent liquid scintillation counting, uptake of [^{3}H]MTX or [^{3}H]cGMP into membrane vesicles was studied by measuring radioactivity associated with the filters. In control experiments, ATP was substituted with AMP. Net ATP-dependent transport was calculated by subtracting values measured in the presence of AMP from those measured in the presence of ATP. Each experi-

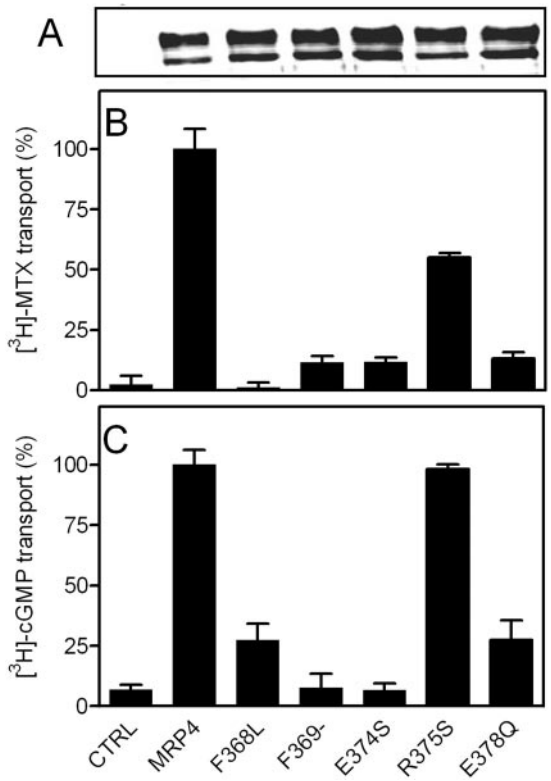

Fig. 3. Western blot analysis (A), 0.5 μM [^{3}H]MTX (B), and 1 μM [^{3}H]cGMP (C) transport activity of wild-type, F368L, F369-, E374S, R375S, and E378Q MRP4 transporter proteins. A, top, Western blot of membrane vesicles isolated from HEK293 cells overexpressing MRP4 or MRP4 mutants F368L, F369-, E374S, R375S, and E378Q, as well as negative control detected by polyclonal anti-human MRP4 (representative of three). The MRP4 wild-type transport activity for [^{3}H]MTX (970 ± 80 fmol/mg protein/min) and [^{3}H]cGMP (106 ± 7 fmol/mg protein/min) was set at 100%.

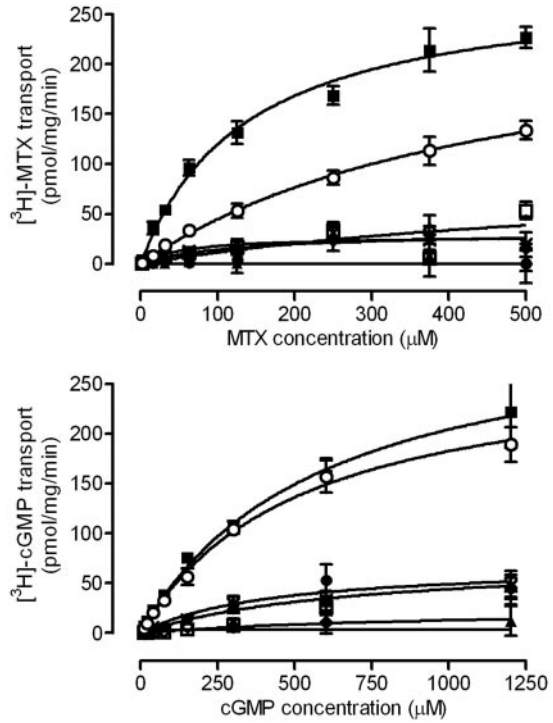

Fig. 4. Concentration-dependent uptake of [^{3}H]MTX and [^{3}H]cGMP in membrane vesicles expressing human MRP4 mutants. Control (▲), wild-type (■), F368L (●), F369- (□), E374S (◇), R375S (○), and E378Q (x) MRP4 membrane vesicles were incubated with [^{3}H]MTX (top) or [^{3}H]cGMP (bottom) concentrations indicated in the figure. ATP-dependent uptake was measured by subtracting uptake in the presence of AMP from that measured in the presence of ATP. Mean values ± S.E. of three enzyme preparations are shown.

ment was performed in triplicate using three different batches of membrane vesicles.

Vesicular Inhibition Assays. To evaluate the inhibitory effects of MTX on [^{3}H]cGMP uptake in MRP4 and MRP4-R375S membrane vesicles, the previously mentioned transport assay was performed using 1, 10, and 100 μM cGMP, in the absence or presence of MTX concentrations ranging from 1 to 600 μM. Net MRP4- or MRP4 mutant-dependent transport was calculated by subtracting background values measured in EYFP-transfected control vesicles.

Kinetic Analysis. All data were expressed as means ± S.D. Curve fitting of the resulting concentration-dependent transport curves was performed by nonlinear regression analysis using GraphPad Prism software, version 4.03 (GraphPad Software Inc., San Diego, CA). Results of the inhibition assays were analyzed using Dixon's method, to estimate the inhibitory potency (K_i).

Immunoprecipitation and Photoaffinity Labeling. Wild-type MRP4, negative (EYFP) control, and mutants (300 μg of protein vesicles) were incubated with 5 mM $MgCl_2$ and 100 μM 8-azido-ATP-biotin (Schäfer et al., 2001) for 5 min on ice. The mixture was photolinked using UV light for 10 min. Immunoprecipitation of the photolinked sample was performed using MRP4 polyclonal antibody (10 μl/sample) (van Aubel et al., 2002) linked to protein A immobilized on agarose [50% (w/v); KemEnTec, Copenhagen, Denmark] (30 μl/sample). The immunoprecipitated protein was blotted (see Western Blotting) and visualized with streptavidin horseradish peroxidase.

Molecular Modeling of MRP4. The homology model of MRP4 was built with the YASARA molecular modeling program (Krieger et al., 2002). A common problem when building models of membrane proteins is the limited availability of experimental data. For MRP4, the related X-ray structure of MsbA seemed to be incorrect and was retracted, which left the structure of the bacterial ABC transporter Sav1866 from *Staphylococcus aureus* solved at 3.0-Å resolution (Dawson and Locher, 2006) as the only available template for the transmembrane domain (PDB entry 2HYD). The cytosolic ATP-binding domain is, in contrast, well represented in the PDB. We therefore selected the more closely related ATP-binding domain from human MDR1 solved at 1.5-Å resolution (Ramaen et al., 2006), aligned it to Sav1866 with YASARA's MUSTANG module (Konagurthu et al., 2006), and then fused it with the Sav1866 transmembrane domain to create a hybrid-template. The alignment of the MRP4 sequence against this template was created with the T-Coffee multiple alignment algorithm (Notredame et al., 2000), using an additional 48 intermediate sequences to guide the alignment. These 48 sequences were randomly selected from Swissprot/TrEMBL, with the requirement that their transmembrane domains be closer to both the template and MRP4, than the template is to MRP4. The resulting alignment was manually tuned to account for single residue insertions and deletions in the membrane helices, which contain several Gly/Pro-mediated deviations from ideality in the Sav1866 template. Loops were modeled by scanning a nonredundant subset of the PDB (>8000 structures) for fragments with matching anchor points, a minimal number of bumps, and maximal sequence similarity. Side chains were added with YASARA's implementation of SCWRL (Canutescu et al., 2003), and then the model was subjected to an energy minimization with the YAMBER force field as described previously (Krieger et al., 2004, 2006). Since no membrane was present during this minimization, the backbone of residues copied from the template was kept fixed. Validation of the model with WHAT_CHECK (Hooft et al., 1996) yielded an average quality Z-score of −2.2, which is

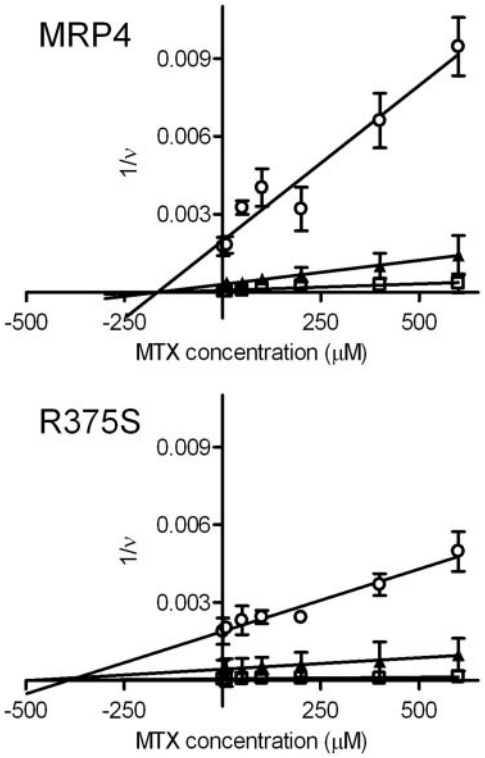

Fig. 5. Dixon plot showing the MTX inhibition of cGMP transport by human MRP4 and mutant R375S. Membrane vesicles were incubated with 1 μM (open circles), 10 μM (closed triangles), or 100 μM (open squares) [^{3}H]cGMP in the presence or absence of MTX concentrations ranging from 1 to 600 μM. Specific uptake of MRP4 (top) and mutant R375S (bottom) was determined after subtraction of the negative control. The inhibition constant (K_i) can be estimated from the intersection point of the three lines with the *x*-axis. Mean values ± S.E. of three enzyme preparations are shown.

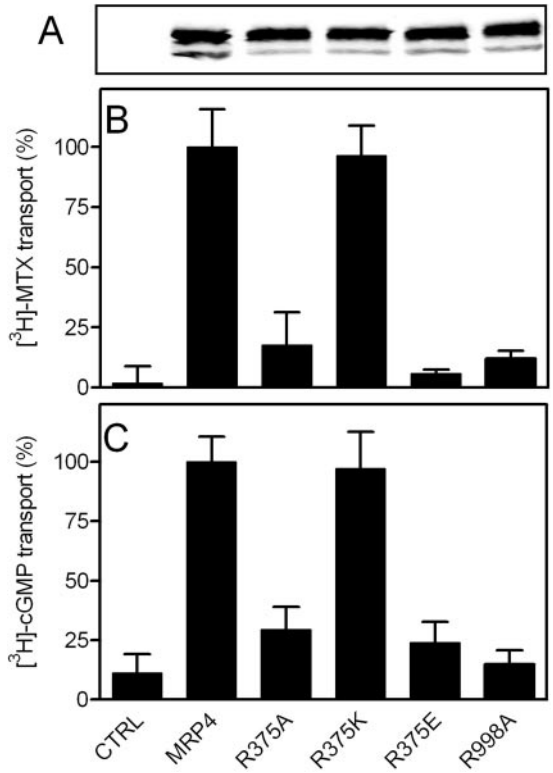

Fig. 6. Western blot analysis (A), 0.5 μM [^{3}H]MTX (B), and 1 μM [^{3}H]cGMP (C) transport activity of wild-type, R375A, R375K, R375E, and R998A MRP4 transporter proteins. A, top, Western blot of membrane vesicles isolated from HEK293 cells overexpressing MRP4 or MRP4 mutants R375A, R375K, R375E, and R998A, as well as negative control detected by polyclonal anti-human MRP4 (representative of three). The MRP4 wild-type transport activity for [^{3}H]MTX (980 ± 20 fmol/mg protein/min) and [^{3}H]cGMP (125 ± 13 fmol/mg protein/min) was set at 100%.

better than the template (−2.9). A PDB file of the model and the alignment is available from us upon request.

Results

Three mutants of human MRP4 were generated and expressed in HEK293 cells. In mutant FF/L-, Phe^{368} and Phe^{369} in TM6 were replaced by their analogs in MRP1/MRP2 (Leu and nothing, respectively). In the second mutant, ERE/SSQ, Glu^{374}, Arg^{375}, and Glu^{378} in TM6 were also replaced by their analogs in MRP1/MRP2 (Ser, Ser, and Gln, respectively). The final mutant FFERE/L-SSQ was a combination of mutant FF/L- and mutant ERE/SSQ. Western blot analysis of membrane vesicles prepared from HEK293 cells overexpressing wild-type MRP4, and the three mutants showed comparable expression levels (Fig. 2A). Often two bands are visible, of which the mutual ratio varies in different preparations.

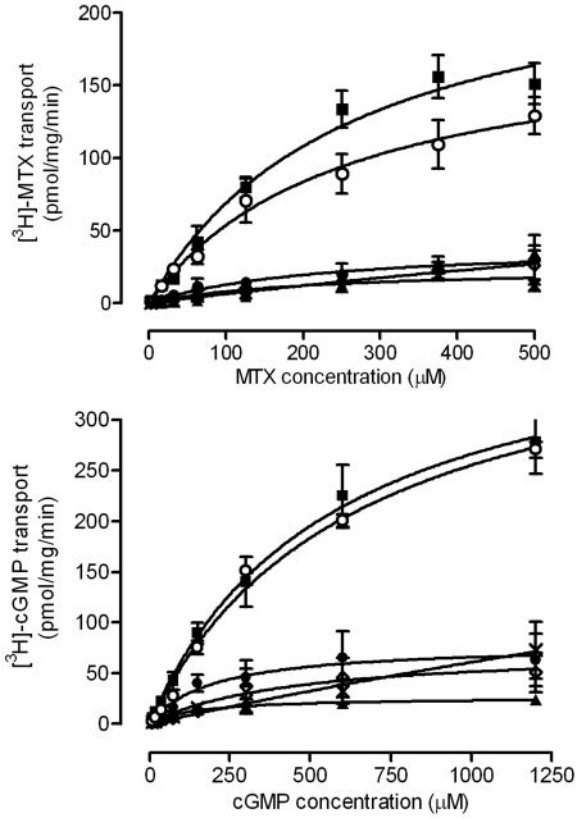

Fig. 7. Concentration-dependent uptake of [^{3}H]MTX and [^{3}H]cGMP in membrane vesicles expressing human MRP4 mutants. Control (▲), wild-type (■), R375A (●), R375K (○), R375E (◇), and R998A (x) MRP4 membrane vesicles were incubated with [^{3}H]MTX (top) or [^{3}H]cGMP (bottom) concentrations indicated in the figure. ATP-dependent uptake was measured by subtracting uptake in the presence of AMP from that measured in the presence of ATP. Mean values ± S.E. of three enzyme preparations are shown.

N-Glycosidase F treatment showed that the most intense band that runs at 170 kDa is the glycosylated MRP4 protein, and the band that runs at 140 kDa is the unglycosylated MRP4 band (data not shown). MRP4-mediated ATP-dependent transport of 0.5 μM [^{3}H]MTX or 1 μM [^{3}H]cGMP was 950 ± 60 and 114 ± 7 pmol/mg protein/min, respectively. In Fig. 2B, the transport activity of the mutants is compared with that of the wild type. Transport of both substrates in all mutants was significantly decreased compared with that of the wild-type transporter. Moreover, the transport activity levels were comparable with that of the negative control.

To investigate the substitution of the amino acids of the previous mutants in more detail, we constructed the single mutants F368L, F369-, E374S, R375S, and E378Q. Again, the membrane vesicles of all mutants showed expression levels comparable with wild-type MRP4 (Fig. 3A). The transport activity of both [^{3}H]MTX and [^{3}H]cGMP (0.5 and 1 μM, respectively) was significantly reduced in mutants F368L, F369-, E374S, and E378Q compared with wild-type MRP4 (Fig. 3). Interestingly, cGMP transport activity of mutant R375S was 98 ± 2% of wild type, whereas its MTX transport activity was only 55 ± 2%.

Next, we determined the transport activity of the mutants and wild-type transporter at different substrate concentrations. Figure 4 shows the Michaelis-Menten plot for MTX and cGMP. Mutants F368L, F369-, E374S, and E378Q showed transport activity levels that were comparable with that of the negative control at all concentrations tested for both MTX and cGMP. The maximum transport rate (V_{max}) values for the wild-type and R375S mutant were 280 ± 60 and 270 ± 120 pmol/mg protein/min for MTX and 370 ± 30 and 270 ± 70 pmol/mg protein/min for cGMP, respectively. The apparent affinity (K_m) values of wild-type MRP4 and mutant R375S were 230 ± 90 and 720 ± 320 μM for MTX and 610 ± 70 and 610 ± 80 μM for cGMP, respectively. The K_m value for cGMP was not influenced by substitution of Arg^{375} with Ser, whereas it was increased 3-fold for MTX.

To test the interaction of MTX and cGMP in more detail, we analyzed the possible inhibitory effect of MTX on [^{3}H]cGMP uptake for wild-type and R375S mutant MRP4. A Dixon plot of net cGMP transport by wild type and R375S in the absence or presence of increasing MTX concentrations was constructed and analyzed by linear regression (Fig. 5). Remarkably, the intersection of the three lines representing MTX inhibition curves at different cGMP concentrations was at the *x*-axis for both wild type and R375S mutant, indicating a noncompetitive inhibitory effect. The inhibition constant value (intersection with the *x*-axis), K_i, for wild-type MRP4 was 164 ± 4 μM, compared with 470 ± 70 μM for mutant R375S.

At this point, however, it was not clear whether this effect was due to the introduction of a polar serine or to the deletion

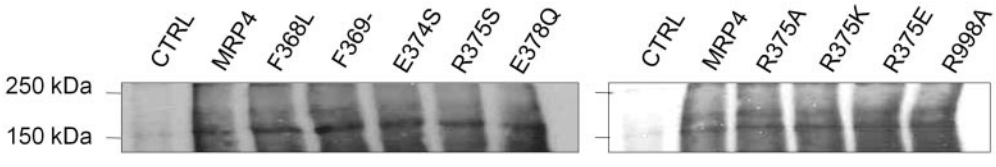

Fig. 8. Western blot of immunoprecipitated 8-azido-ATP-biotin photolabeled wild-type and mutant transporter proteins. We labeled 300 μg of protein vesicles with 100 μM 8-azido-ATP-biotin, and the MRP4 proteins were immunoprecipitated with MRP4 polyclonal antibody linked to agarose protein A beads. The immunoprecipitated protein was blotted and visualized with streptavidin horseradish peroxidase. The addition of 5 mM ATP prevented photolabeling (data not shown).

of the positively charged arginine. In the next experiment, we replaced arginine with alanine, lysine, and glutamic acid. Furthermore, we substituted the arginine present in TM12 for alanine. Figure 6A shows an equal level of protein expression of wild type as well as R375A, R375K, R375E, and R988A mutants. The MTX and cGMP transport activity of the wild-type and mutants was measured and shown in Fig. 6B. Mutating the Arg^{375} residue into alanine or glutamic acid significantly decreased the transport activity for both MTX and cGMP, whereas mutating it into lysine retained the transport activity (96 ± 12% for MTX and 97 ± 16% for cGMP). In addition, the transport levels of R988A showed no significant difference from the negative control.

To determine the K_m values of the different mutants for MTX and cGMP, concentration-dependent transport experiments were performed (Fig. 7). The transport activities of R375A, R375E, and R988A for MTX and cGMP did not differ from that of the negative control. The V_{max} values for MTX were 250 ± 20 and 190 ± 10 pmol/mg protein/min and those for cGMP were 420 ± 10 and 420 ± 20 pmol/mg protein/min for wild type and R375S mutant, respectively. The K_m values of wild-type MRP4 and R375K were 230 ± 90 and 250 ± 20 μM for MTX and 610 ± 70 and 640 ± 60 μM for cGMP, respectively. Thus, R375K retained substrate affinity comparable with the wild type for both MTX and cGMP.

To determine whether the MRP4 mutants showed normal ATP binding, 8-azido-ATP-biotin photolabeling of mutants was compared with that of wild type and negative control (Fig. 8). The vesicles of MRP4 wild type and mutants showed increased 8-azido-ATP-biotin binding compared with the negative control. In all mutant preparations, the 8-azido-ATP-biotin binding was comparable with that of the wild type. Moreover, the binding of 8-azido-ATP-biotin was almost completely diminished when ATP was added.

To link the functional consequences of the mutations back to their structural basis, we built a homology model of MRP4 using the known X-ray structures of the bacterial ABC transporter Sav1866 from *S. aureus* (Dawson and Locher, 2006) and the ATP-binding domain of human P-glycoprotein/MDR1 as templates (Ramaen et al., 2006) (Fig. 9A). Sav1866 forms a dimer, whereas MRP4 encodes both copies in a single sequence. The predicted location of the mutated residues is shown in Fig. 9B. Based on this model, one can postulate that Arg^{375} and Arg^{998} face right into the pore and are thus very likely to interact directly with MTX and cGMP.

Discussion

To characterize the MRP4 substrate-binding site, we investigated the influence of Phe^{368}, Phe^{369}, Glu^{374}, Arg^{375}, and Glu^{378} of transmembrane helix 6 and the influence of Arg^{998} of helix 12 on cGMP and MTX transport. These amino acids were substituted by their corresponding amino acids of MRP1 and MRP2. Most mutations abolished MRP4 transport activity. The only exception was substitution of Arg^{375} with serine, which had no effect on cGMP transport, but significantly decreased the affinity for MTX. Substitution of the same amino acid with a positively charged lysine returned the MTX affinity to that of the wild type. A homology model of MRP4 confirmed the crucial role of Arg^{375} and showed that it faced right into the central pore.

Wild-type MRP4 and all mutants were equally expressed in vesicles isolated from transduced HEK293 cells. Nevertheless, several MRP4 mutants (FF/L-, ERE/SSQ, FFERE/L-SSQ, F368L, F369-, E374S, R375A, R375E, E378Q, and R998A) showed significantly diminished transport activity of either MTX or cGMP compared with that of wild-type MRP4. This indicates that Phe^{368}, Phe^{369}, Glu^{374}, Arg^{375}, and Glu^{378}, present in TM6, and Arg^{998}, present in TM12, might comprise an important part of MRP4 substrate-binding site. Indeed, studies with LmrA, a bacterial ATP-dependent multidrug transporter, show that TM3, TM5, and TM6 (also TM9, TM11, and TM12) are involved in substrate binding (Ecker et al., 2004). These TMs have one face of the helix exposed to the pore, which forms a pathway for substrates through the membrane. Experimental evidence has shown

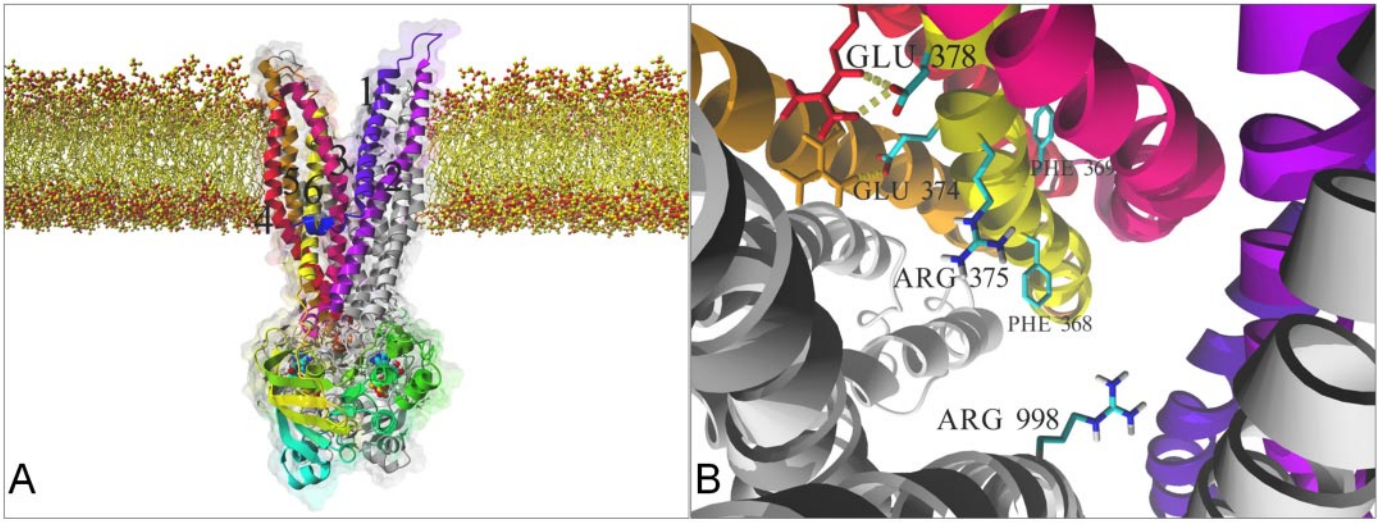

Fig. 9. Homology model of human MRP4 (A). The first half of the protein containing transmembrane helices 1 to 6 and the first ATP-binding domain are colored with a gradient from blue over orange to cyan. The second half of the protein (corresponding to the second monomer in the dimeric Sav1866 modeling template) is shown in gray. A 180° rotation around the vertical axis would yield an almost identical picture of helices 7 to 12 and the second ATP-binding domain. B, close-up of the channel formed by the 12 transmembrane helices, looking from the inside to the extracellular side. The mutants described in this work are indicated. Graphics created with www.YASARA.org.

that conformational changes of the nucleotide-binding domains (NBD) of P-glycoprotein/MDR1, leads to reorientation of the TM helices (Loo et al., 2007). TM6 is connected to NBD1 and changes in the position or orientation of TM6 resulting from mutations, may cause a conformational or positional change in NBD1 leading to diminished binding of ATP and transport activity (Zhang et al., 2004). We tested whether the mutants were able to bind 8-azido-ATP-biotin and observed no difference in binding between MRP4 and the mutants.

All the amino acids mutated in the present study are highly conserved in MRP4 among different species (Chen and Klaassen, 2004). There is, however, a big difference within the MRP subfamily that might point to a specific mechanistic importance of these amino acids. The two phenylalanines at position 368 and 369 in MRP4 are unique and absent in other MRPs. Replacement of these two amino acids by a single leucine (their counterpart in MRP1, -2, -3, and -5) resulted in the lack of MTX and cGMP transport. The Phe^{369}, predicted to face outside the central pore and attach helix 6 to helix 3, most likely has a role in maintaining the structural integrity of the transporter. Phe^{368} faces into the pore and could mediate stacking interactions with the planar rings of cGMP and MTX. The negatively charged glutamic acid residues at position 374 and 378 of MRP4 correspond to a serine and glutamine, respectively, in MRP1, -2, and -6. The replacement of these two MRP4 amino acids by serine and glutamine also resulted in the lack of MTX and cGMP transport. Zhang et al. (2004) showed that replacement of MRP1 Ser^{604} (corresponding to E374S in MRP4) with alanine selectively increased 17β-estradiol 17-(β-D-glucuronide) transport. In the model, Glu^{374} and Glu^{378} form salt bridges with Arg^{317} and Arg^{262}, which points toward a role in maintaining the structural integrity of the transporter.

In this study, we showed that the positively charged arginine residue at position 375 is important for MRP4-mediated MTX but not cGMP transport. The importance of positively charged amino acids to the binding and transport functionality was indicated previously for MRP1 (Zhang et al., 2003a). Deletion of the hydroxyl group of MRP1 residue 605 (S605A), corresponding to R375A in MRP4, decreased resistance to vincristine, etoposide (VP-16), and doxorubicin (Zhang et al., 2004). Moreover, the Q359K/T360K mutation (corresponding to MRP4 Glu^{374} and Arg^{375}) in the cystic fibrosis transmembrane conductance regulator protein causes cystic fibrosis (Quint et al., 2005).

In the present study, substitution of MRP4 Arg^{375} with serine resulted in a lower affinity for MTX, but the affinity for cGMP did not change (Table 1). Furthermore, the MTX inhibition constant for cGMP transport by mutant R375S was significantly lower than that of the wild type. When the arginine at position 375 of MRP4 was substituted with lysine, another positively charged amino acid, MTX and cGMP transport activities were similar to that of the MRP4 wild type. For MTX affinity, the positive charge of MRP4 residue 375 is critical. When this charge is removed (R375S), the MTX affinity decreases or transport activity is absent (R375A and R375E). This positive charge is less important for cGMP transport, because in the presence of a hydroxyl group (R375S), the transport properties seem unchanged. As soon as this hydroxyl group is removed (R375A) or replaced with a (negatively charged) acidic group (R375E), transport of cGMP is absent. Our observation that the R375S mutation has a larger effect on MTX transport could be explained by the fact that MTX contains two negative charges that need to be compensated, whereas cGMP only has one. Regardless, our results show that lysine is equally well suited as arginine to mediate this interaction.

TABLE 1
Transporter kinetic values and inhibition constants

	MTX		cGMP		
	K_m	V_{max}	K_m	V_{max}	K_i
	μM	$pmol/mg/min$	μM	$pmol/mg/min$	μM
Data from Figs. 3 and 4					
MRP4	230 ± 90	280 ± 60	610 ± 70	370 ± 30	164 ± 4
R375S	720 ± 320	270 ± 120	610 ± 80	270 ± 70	470 ± 70
Data from Fig. 4					
MRP4	230 ± 90	250 ± 20	610 ± 70	420 ± 10	
R375K	250 ± 20	190 ± 10	640 ± 60	420 ± 20	

Photolabeling and mutational studies aimed at predicting regions of MRP1 protein that contribute to the substrate-binding sites have outlined the possible role of TM17 (Daoud et al., 2001; Deeley et al., 2006), which corresponds to TM12 in MRP4. In the present work, we mutated Arg^{998} located at MRP4 TM12 into alanine. Substitution of this positively charged amino acid resulted in near abolition of transport activity for either MTX or cGMP. It was reported that the corresponding amino acid Arg^{1257} in MRP2 showed decreased transport activity of glutathione-methylfluorescein when substituted with alanine (Ryu et al., 2000). Moreover, alanine substitution of Arg^{1249} in MRP1 (also corresponding to R998A) impaired MRP1-mediated LTC4 transport and reduced vincristine resistance (Ren et al., 2002). This indicates the participation of TM12 to the MRP4 binding pocket and emphasizes the importance of positively charged amino acids for MRP4 transport activity. Although mutagenesis studies confirm the functional requirement of a positive charge at Arg^{375}, this has not been confirmed for Arg^{998}. Glutamic acid (R998E) and lysine (R998K) mutants would be needed to strengthen this conclusion.

Complex substrate-transporter interactions have been described previously for ABC transporters such as P-glycoprotein/MDR1 (Martin et al., 2000), MRP1 (Leslie et al., 2001), MRP2 (Zelcer et al., 2003), and MRP4 (Van Aubel et al., 2005). These complexities were attributed to multiple allosteric-binding sites. Here, we encountered similar complex transport inhibition patterns. Mutant R375S and wild-type MRP4 possessed similar affinities for cGMP, but the MTX affinity of this mutant was nearly 3-fold lower than that of the wild type. This implicates that these two MRP4 substrates do not share the same substrate-binding site. This was also implied by the noncompetitive inhibitory effect of MTX on MRP4-mediated cGMP transport. Therefore, we propose that MRP4 can bind two substrates at different regions within the aqueous cavity involving overlapping amino acids. This could partly explain the complex inhibitory and stimulatory kinetics that we encountered in previous studies (Van Aubel et al., 2005; El-Sheikh et al., 2007). Our data are indicative; they are nonetheless based on a homology model and mutagenesis studies, both of which contain certain experimental caveats.

We conclude that amino acids in the transmembrane helices 6 and 12 may comprise a crucial part of the MRP4

substrate-binding site. The importance of a positive charge at residue 375 seems evident for MTX transport, but not for cGMP. This residue, which is predicted to be in the aqueous cavity of the inner leaflet of the membrane, clearly affects substrate specificity. Furthermore, a noncompetitive inhibition between MTX and cGMP has been revealed, indicating separate MRP4 substrate-binding sites.

Acknowledgments

We thank M. van Hout for technical assistance in the vesicular transport assays.

References

Borst P, de Wolf C, and van de Wetering K (2007) Multidrug resistance-associated proteins 3, 4, and 5. *Pflugers Arch* **453:**661–673.

Canutescu AA, Shelenkov AA, and Dunbrack RL Jr (2003) A graph-theory algorithm for rapid protein side-chain prediction. *Protein Sci* **12:**2001–2014.

Chen C and Klaassen CD (2004) Rat multidrug resistance protein 4 (Mrp4, Abcc4): molecular cloning, organ distribution, postnatal renal expression, and chemical inducibility. *Biochem Biophys Res Commun* **317:**46–53.

Chen ZS, Lee K, Walther S, Raftogianis RB, Kuwano M, Zeng H, and Kruh GD (2002) Analysis of methotrexate and folate transport by multidrug resistance protein 4 (ABCC4): MRP4 is a component of the methotrexate efflux system. *Cancer Res* **62:**3144–3150.

Daoud R, Julien M, Gros P, and Georges E (2001) Major photoaffinity drug binding sites in multidrug resistance protein 1 (MRP1) are within transmembrane domains 10-11 and 16-17. *J Biol Chem* **276:**12324–12330.

Dawson RJ and Locher KP (2006) Structure of a bacterial multidrug ABC transporter. *Nature* **443:**180–185.

Deeley RG, Westlake C, and Cole SP (2006) Transmembrane transport of endo- and xenobiotics by mammalian ATP-binding cassette multidrug resistance proteins. *Physiol Rev* **86:**849–899.

Ecker GF, Pleban K, Kopp S, Csaszar E, Poelarends GJ, Putman M, Kaiser D, Konings WN, and Chiba P (2004) A three-dimensional model for the substrate binding domain of the multidrug ATP binding cassette transporter LmrA. *Mol Pharmacol* **66:**1169–1179.

El-Sheikh AA, van den Heuvel JJ, Koenderink JB, and Russel FG (2007) Interaction of nonsteroidal anti-inflammatory drugs with multidrug resistance protein (MRP) 2/A. *J Pharmacol Exp Ther* **320:**229–235.

Hooft RW, Vriend G, Sander C, and Abola EE (1996) Errors in protein structures. *Nature* **381:**272.

Ito K, Oleschuk CJ, Westlake C, Vasa MZ, Deeley RG, and Cole SP (2001a) Mutation of Trp1254 in the multispecific organic anion transporter, multidrug resistance protein 2 (MRP2) (ABCC2), alters substrate specificity and results in loss of methotrexate transport activity. *J Biol Chem* **276:**38108–38114.

Ito K, Olsen SL, Qiu W, Deeley RG, and Cole SP (2001b) Mutation of a single conserved tryptophan in multidrug resistance protein 1 (MRP1/ABCC1) results in loss of drug resistance and selective loss of organic anion transport. *J Biol Chem* **276:**15616–15624.

Koike K, Conseil G, Leslie EM, Deeley RG, and Cole SP (2004) Identification of proline residues in the core cytoplasmic and transmembrane regions of multidrug resistance protein 1 (MRP1/ABCC1) important for transport function, substrate specificity, and nucleotide interactions. *J Biol Chem* **279:**12325–12336.

Konagurthu AS, Whisstock JC, Stuckey PJ, and Lesk AM (2006) MUSTANG: a multiple structural alignment algorithm. *Proteins* **64:**559–574.

Krieger E, Darden T, Nabuurs SB, Finkelstein A, and Vriend G (2004) Making optimal use of empirical energy functions: force-field parameterization in crystal space. *Proteins* **57:**678–683.

Krieger E, Koraimann G, and Vriend G (2002) Increasing the precision of comparative models with YASARA NOVA–a self-parameterizing force field. *Proteins* **47:**393–402.

Krieger E, Nielsen JE, Spronk CA, and Vriend G (2006) Fast empirical PKa prediction by Ewald summation. *J Mol Graph Model* **25:**481–486.

Laemmli UK (1970) Cleavage of structural proteins during the assembly of the head of bacteriophage T4. *Nature* **227:**680–685.

Leslie EM, Ito K, Upadhyaya P, Hecht SS, Deeley RG, and Cole SP (2001) Transport of the β-O-glucuronide conjugate of the tobacco-specific carcinogen 4-(methylnitrosamino)-1-(3-pyridyl)-1-butanol (NNAL) by the multidrug resistance protein 1 (MRP1). Requirement for glutathione or a non-sulfur-containing analog. *J Biol Chem* **276:**27846–27854.

Loo TW, Bartlett MC, and Clarke DM (2007) Nucleotide binding, ATP hydrolysis, and mutation of the catalytic carboxylates of human p-glycoprotein cause distinct conformational changes in the transmembrane segments. *Biochemistry* **46:**9328–9336.

Martin C, Berridge G, Higgins CF, Mistry P, Charlton P, and Callaghan R (2000) Communication between multiple drug binding sites on P-glycoprotein. *Mol Pharmacol* **58:**624–632.

Notredame C, Higgins DG, and Heringa J (2000) T-Coffee: a novel method for fast and accurate multiple sequence alignment. *J Mol Biol* **302:**205–217.

Quint A, Lerer I, Sagi M, and Abeliovich D (2005) Mutation spectrum in Jewish cystic fibrosis patients in Israel: implication to carrier screening. *Am J Med Genet A* **136:**246–248.

Ramaen O, Leulliot N, Sizun C, Ulryck N, Pamlard O, Lallemand JY, Tilbeurgh H, and Jacquet E (2006) Structure of the human multidrug resistance protein 1 nucleotide binding domain 1 bound to Mg2+/ATP reveals a non-productive catalytic site. *J Mol Biol* **359:**940–949.

Ren XQ, Furukawa T, Aoki S, Sumizawa T, Haraguchi M, Nakajima Y, Ikeda R, Kobayashi M, and Akiyama S (2002) A positively charged amino acid proximal to the C-terminus of TM17 of MRP1 is indispensable for GSH-dependent binding of substrates and for transport of LTC4. *Biochemistry* **41:**14132–14140.

Russel FG, Koenderink JB, and Masereeuw R (2008) Multidrug resistance protein 4 (MRP4/ABCC4): a versatile efflux transporter for drugs and signalling molecules. *Trends Pharmacol Sci* **29:**200–207.

Ryu S, Kawabe T, Nada S, and Yamaguchi A (2000) Identification of basic residues involved in drug export function of human multidrug resistance-associated protein 2. *J Biol Chem* **275:**39617–39624.

Schäfer HJ, Coskun U, Eger O, Godovac-Zimmermann J, Wieczorek H, Kagawa Y, and Grüber G (2001) 8-N(3)-3′-Biotinyl-ATP, a novel monofunctional reagent: differences in the F(1)- and V(1)-ATPases by means of the ATP analogue. *Biochem Biophys Res Commun* **286:**1218–1227.

Schuetz JD, Connelly MC, Sun D, Paibir SG, Flynn PM, Srinivas RV, Kumar A, and Fridland A (1999) MRP4: a previously unidentified factor in resistance to nucleoside-based antiviral drugs. *Nat Med* **5:**1048–1051.

van Aubel RA, Smeets PH, Peters JG, Bindels RJ, and Russel FG (2002) The MRP4/ABCC4 gene encodes a novel apical organic anion transporter in human kidney proximal tubules: putative efflux pump for urinary CAMP and CGMP. *J Am Soc Nephrol* **13:**595–603.

Van Aubel RA, Smeets PH, van den Heuvel JJ, and Russel FG (2005) Human organic anion transporter MRP4 (ABCC4) is an efflux pump for the purine end metabolite urate with multiple allosteric substrate binding sites. *Am J Physiol Renal Physiol* **288:**F327–F333.

van de Water FM, Masereeuw R, and Russel FG (2005) Function and regulation of multidrug resistance proteins (MRPs) in the renal elimination of organic anions. *Drug Metab Rev* **37:**443–471.

Wielinga PR, Reid G, Challa EE, van der Heijden I, van Deemter L, de Haas M, Mol C, Kuil AJ, Groeneveld E, Schuetz JD, et al. (2002) Thiopurine metabolism and identification of the thiopurine metabolites transported by MRP4 and MRP5 overexpressed in human embryonic kidney cells. *Mol Pharmacol* **62:**1321–1331.

Zelcer N, Huisman MT, Reid G, Wielinga P, Breedveld P, Kuil A, Knipscheer P, Schellens JH, Schinkel AH, and Borst P (2003) Evidence for two interacting ligand binding sites in human multidrug resistance protein 2 (ATP binding cassette C2). *J Biol Chem* **278:**23538–23544.

Zhang DW, Cole SP, and Deeley RG (2001) Identification of a nonconserved amino acid residue in multidrug resistance protein 1 important for determining substrate specificity: evidence for functional interaction between transmembrane helices 14 and 17. *J Biol Chem* **276:**34966–34974.

Zhang DW, Gu HM, Situ D, Haimeur A, Cole SP, and Deeley RG (2003a) Functional importance of polar and charged amino acid residues in transmembrane helix 14 of multidrug resistance protein 1 (MRP1/ABCC1): identification of an aspartate residue critical for conversion from a high to low affinity substrate binding state. *J Biol Chem* **278:**46052–46063.

Zhang DW, Gu HM, Vasa M, Muredda M, Cole SP, and Deeley RG (2003b) Characterization of the role of polar amino acid residues within predicted transmembrane helix 17 in determining the substrate specificity of multidrug resistance protein 3. *Biochemistry* **42:**9989–10000.

Zhang DW, Nunoya K, Vasa M, Gu HM, Cole SP, and Deeley RG (2006) Mutational analysis of polar amino acid residues within predicted transmembrane helices 10 and 16 of multidrug resistance protein 1 (ABCC1): effect on substrate specificity. *Drug Metab Dispos* **34:**539–546.

Zhang DW, Nunoya K, Vasa M, Gu HM, Theis A, Cole SP, and Deeley RG (2004) Transmembrane helix 11 of multidrug resistance protein 1 (MRP1/ABCC1): identification of polar amino acids important for substrate specificity and binding of ATP at nucleotide binding domain 1. *Biochemistry* **43:**9413–9425.

Address correspondence to: Dr. J. B. Koenderink, Department of Pharmacology and Toxicology (149), Radboud University Nijmegen Medical Centre, Nijmegen Centre for Molecular Life Sciences, P.O. Box 9101, 6500 HB Nijmegen, The Netherlands. E-mail: j.koenderink@ncmls.ru.nl.